Advances in Pure Mathematics, 2022, 12, 465-477
https://www.scirp.org/journal/apm
ISSN Online: 2160-0384
ISSN Print: 2160-0368

# Phase Portraits and Traveling Wave Solutions of a Fractional Generalized Reaction Duffing Equation

**Kelei Zhang*, Zhenfeng Zhang, Tao Yuwen**

School of Mathematics and Computing Science, Guilin University of Electronic Technology, Guilin, China
Email: *keleizhang@163.com, zhangzhenfengzzf@126.com, 2269728037@qq.com

**How to cite this paper:** Zhang, K.L., Zhang, Z.F. and Yuwen, T. (2022) Phase Portraits and Traveling Wave Solutions of a Fractional Generalized Reaction Duffing Equation. *Advances in Pure Mathematics*, **12**, 465-477.
https://doi.org/10.4236/apm.2022.127035

**Received:** July 5, 2022
**Accepted:** July 25, 2022
**Published:** July 28, 2022



## Abstract

In this paper, we study the traveling wave solutions of the fractional generalized reaction Duffing equation, which contains several nonlinear conformable time fractional wave equations. By the dynamic system method, the phase portraits of the fractional generalized reaction Duffing equation are given, and all possible exact traveling wave solutions of the equation are obtained.

## Keywords

Fractional Duffing Equation, Dynamic System Method, Traveling Wave Solution

## 1. Introduction

Some famous nonlinear fractional wave equations, such as the fractional Klein-Gordon equation, Landau-Ginzburg-Higgs equation, the fractional $\varphi^4$ equation, the fractional Duffing equation and the fractional Sine-Gordon equation, can be summarized as the fractional generalized reaction Duffing model. A lot of authors have done a lot of research on the exact solutions of this equation. By using the new ansatz method, the solitary wave solutions and periodic solutions of gRDM were obtained in [1]. Furthermore, the exact soliton solutions of gRDM have been obtained by using the generalized hyperbolic function method, the Bäcklund transformation obtained by the homogeneous balance method, the first integration method of the fractional derivative in the sense of the improved Riemann-Liouville derivative, and the compatible fractional complex transformation method, respectively in [2] [3] [4] [5]. Based on an extended first-type elliptic sub-equation method and its algorithm, the new bell-shaped and kink-shaped solitary wave solutions, triangular periodic wave solutions and singular solutions of gRDM were solved in [6]. The accurate soliton solutions were obtained by using Bäcklund transformation of fractional Riccati equation, function variable method, and general projective Riccati equation [7] [8] [9]. In addition, other authors have used auxiliary function methods, Hermite transformation and Riccati equations, fractional sub-equations and other methods to study the exact solutions of gRDM in [10] [11] [12]. Recently, some new traveling wave solutions of the (2+1)-dimensional time-fractional Zoomeron equation and the superfield gardner equation have been obtained in [13] [14]. The fractional derivatives and fractional derivative equations have been deeply studied in [15] [16] [17] [18]. In this paper, we consider the following fractional order generalized reaction Duffing equation

$$D_t^{2\alpha}u + pu_{xx} + qu + ru^2 + su^3 = 0, \tag{1}$$

where $p, q, r$ and $s$ are all real constants, $0 < \alpha \le 1$, and $D_t^{2\alpha} = D_t^{\alpha} D_t^{\alpha}$ is defined in Section 2. The following equations are special cases of Equation (1), for example

1) Fractional Klein-Gordon equation

$$D_t^{2\alpha}u - u_{xx} - au - bu^3 = 0, t > 0, 0 < \alpha \le 1.$$

2) Fractional Landau-Ginzburg-Higgs equation

$$D_t^{2\alpha}u - u_{xx} - m^2u + gu^3 = 0, t > 0, 0 < \alpha \le 1.$$

3) Fractional $\varphi^4$ equation

$$D_t^{2\alpha}u - u_{xx} + u - u^3 = 0, t > 0, 0 < \alpha \le 1.$$

4) Fractional Duffing equation

$$D_t^{2\alpha}u + au + bu^3 = 0, t > 0, 0 < \alpha \le 1.$$

5) Fractional Sine-Gordon equation

$$D_t^{2\alpha}u + au + bu^3 = 0, t > 0, 0 < \alpha \le 1.$$

In this paper, we use the dynamic system approach [19] [20] to study the phase portraits and traveling wave solutions of the Equation (1), and try to construct all possible exact traveling wave solutions of this equation.

The rest of this paper is organized as follows. In Section 2, we introduce some basic definitions and important properties of the fractional derivative. In Section 3, by applying the dynamic system approach [19] [20], we give the phase portraits of the Equation (1). In Section 4, we give all possible exact traveling wave solutions of the Equation (1) under different parameters. In Section 5, we state the main conclusions of this paper.

## 2. Definition and Properties of the Fractional Derivative

The idea of fractional derivatives originated from the semi-derivative discussed by Leibniz and Lopida in 1695. Subsequently, many authors studied fractional derivatives and formed several different definitions, such as Riemann-Liouville, Caputo and other fractional derivatives. In this section, we introduce the common fractional derivatives proposed by Khalil *et al.* [21]. Let $f:(0,+\infty)\to\mathbf{R}$. Then, the conformal fractional derivative of $f$ of order $\alpha$ is defined as

$$D_t^{\alpha} f(t)=\lim_{\varepsilon\to 0}\frac{f\left(t+\varepsilon t^{1-\alpha}\right)-f(t)}{\varepsilon}, \tag{2}$$

for all $t>0$, $\alpha\in(0,1]$. And the conformal fractional derivative has the following properties. Let $\alpha\in(0,1]$, and $f,g$ be $\alpha$-differentiable at a point $t>0$. Then

$$\begin{aligned}&D_t^{\alpha} t^s=st^{s-\alpha}, s\in\mathbf{R},\\&D_t^{\alpha}\left[f(t)g(t)\right]=g(t)D_t^{\alpha}f(t)+f(t)D_t^{\alpha}g(t).\end{aligned} \tag{3}$$

In addition, if $f$ is differentiable, then

$$D_t^{\alpha} f(t)=t^{1-\alpha}\frac{\mathrm{d}f(t)}{\mathrm{d}t}. \tag{4}$$

## 3. Phase Portraits of Equation (1)

Inspired by [22], we introduce the following fractional transformation

$$\xi=kx-\frac{n}{\alpha}t^{\alpha}, U(\xi)=u(t,x), \tag{5}$$

where $k,n$ are all arbitrary constants. According to (3)-(4), it infers

$$D_t^{\alpha}D_t^{\alpha}u(t)=D_t^{\alpha}\left(t^{1-\alpha}\frac{\mathrm{d}U(\xi)}{\mathrm{d}\xi}\cdot\frac{\mathrm{d}\xi}{\mathrm{d}t}\right)=D_t^{\alpha}\left(-n\frac{\mathrm{d}U(\xi)}{\mathrm{d}\xi}\right)=n^2\frac{\mathrm{d}^2U(\xi)}{\mathrm{d}\xi^2}. \tag{6}$$

By (6), substituting Equation (5) into Equation (1), we get

$$\left(n^2+pk^2\right)U''+qU+rU^2+sU^3=0, \tag{7}$$

where $'$ is the derivative with respect to $\xi$. Furthermore, it follows from [20] [23] that (7) is equivalent to the plane Hamiltonian system

$$\begin{aligned}&\frac{\mathrm{d}U}{\mathrm{d}\xi}=V,\\&\frac{\mathrm{d}V}{\mathrm{d}\xi}=AU^3+BU^2+PU,\end{aligned} \tag{8}$$

with the Hamiltonian

$$H(U,V)=\frac{1}{2}V^2-\frac{A}{4}U^4-\frac{B}{3}U^3-\frac{P}{2}U^2=h,$$

where $A=-\frac{s}{n^2+pk^2}, B=-\frac{r}{n^2+pk^2}, P=-\frac{q}{n^2+pk^2}$.

In order to study the phase pictures of the system (8), it is necessary to study the equilibrium points of the system (8). Let $\Delta=B^2-4AP$. When $\Delta=0$, the system (8) has two equilibrium points $E_0(0,0), E_1(-B/2A,0)$. When $\Delta>0$, the system has three equilibrium points $E_0(0,0), E_2\left(\frac{-B+\sqrt{\Delta}}{2A}\right)$ and $E_3\left(-\frac{B+\sqrt{\Delta}}{2A},0\right)$. When $\Delta<0$, the system has only one equilibrium point

$E_0(0,0)$. Let $M(U_e,V_e)$ be the coefficient matrix of the linearized system of the system (8) at an equilibrium point $E_j\ (j=0,1,2,3)$. Let $J=\det\left(M(U_e,V_e)\right)$. We have

$$
\begin{aligned}
&J(E_0)=-P,\\
&J(E_1)=0,\\
&J(E_2)=\frac{B\sqrt{\Delta}-\Delta}{2A},\\
&J(E_3)=-\frac{B\sqrt{\Delta}+\Delta}{2A},\\
&\operatorname{Trace}\left(M(E_j)\right)=0,(j=0,1,2,3).
\end{aligned}
$$

By the planar dynamical theory [20], the above analysis and Maple, we obtain the following results and the phase portraits.

**Case 1.** $\Delta=0$.

When $P>0$, $E_0(0,0)$ is a saddle point and $E_1\left(-\frac{B}{2A},0\right)$ is a cusp point.

When $P<0$, $E_0(0,0)$ is a center point and $E_1\left(-\frac{B}{2A},0\right)$ is a cusp point.

The corresponding phase portraits of the system (8) are shown in **Figure 1**.

**Case 2.** $\Delta>0$.

When $P>0$, $A>0$ and $B<0$, $E_0(0,0)$ and $E_2\left(\frac{-B+\sqrt{\Delta}}{2A}\right)$ are saddle points and $E_3\left(-\frac{B+\sqrt{\Delta}}{2A},0\right)$ is a center point.

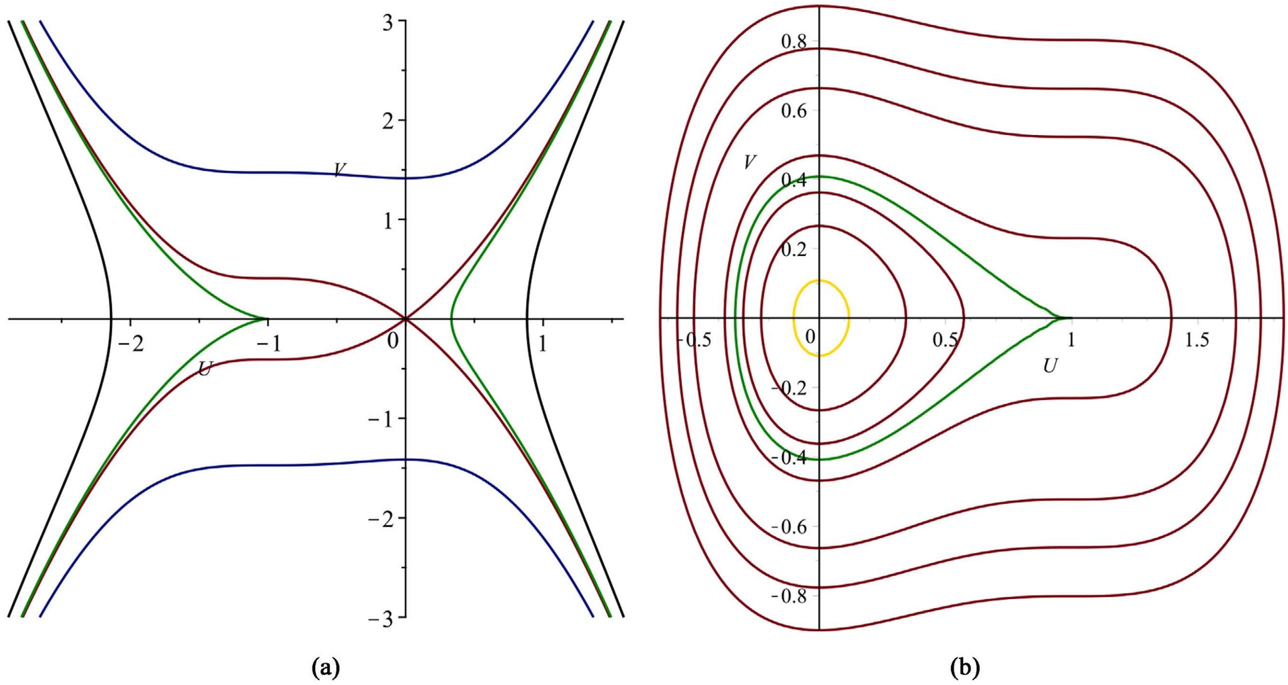


**Figure 1.** The phase portraits of the system (8). (a) $\Delta=0,P>0$; (b) $\Delta=0,P>0$.

When $P>0$, $A>0$ and $B>0$, $E_0(0,0)$ and $E_3\left(-\dfrac{B+\sqrt{\Delta}}{2A},0\right)$ are saddle points and $E_2\left(\dfrac{-B+\sqrt{\Delta}}{2A}\right)$ is a center point.

When $P>0$, $A<0$, $E_0(0,0)$ is a saddle point, and $E_2\left(\dfrac{-B+\sqrt{\Delta}}{2A}\right)$ and $E_3\left(-\dfrac{B+\sqrt{\Delta}}{2A},0\right)$ are center points.

When $P<0$, $A>0$, $E_0(0,0)$ is a center point, and $E_2\left(\dfrac{-B+\sqrt{\Delta}}{2A}\right)$ and $E_3\left(-\dfrac{B+\sqrt{\Delta}}{2A},0\right)$ are saddle points.

When $P<0$, $A<0$ and $B>0$, $E_0(0,0)$ and $E_3\left(-\dfrac{B+\sqrt{\Delta}}{2A},0\right)$ are center points and $E_2\left(\dfrac{-B+\sqrt{\Delta}}{2A}\right)$ is a saddle point.

When $C<0$, $A<0$ and $B<0$, $E_0(0,0)$ and $E_2\left(\dfrac{-B+\sqrt{\Delta}}{2A}\right)$ are center points and $E_3\left(-\dfrac{B+\sqrt{\Delta}}{2A},0\right)$ is a saddle point.

When $C=0$ and $A>0$, $E_0(0,0)$ and $E_2(0,0)$ are cusp points and $E_3\left(-\dfrac{B+\sqrt{\Delta}}{2A},0\right)$ is a saddle point.

When $C=0$ and $A<0$, $E_0(0,0)$ and $E_2(0,0)$ are cusp points and $E_3\left(-\dfrac{B+\sqrt{\Delta}}{2A},0\right)$ is a center point.

The corresponding phase portraits of the system (8) are shown in **Figures 2-6**.

**Case 3.** $\Delta<0$

When $P>0$, $E_0(0,0)$ is a saddle point.

When $P<0$, $E_0(0,0)$ is a center point.

The corresponding phase portraits of the system (8) are shown in **Figure 7**.

## 4. Exact Solutions of Equation (1)

We use the elliptic integral theory and direct integration method to give all possible explicit parameter representations of the traveling wave solution of Equation (1). We first denote

$$h_0=H(0,0)=0,$$

$$h_1=H\left(-\frac{B}{2A},0\right)=\frac{5B^4}{192A^3}-\frac{PB^2}{8A^2},$$

$$h_2 = H\left(\frac{-B+\sqrt{\Delta}}{2A},0\right) = -\frac{3W_1^4+8BW_1^3}{192A^3} - \frac{PW_1^2}{8A^2},$$
$$h_3 = H\left(-\frac{B+\sqrt{\Delta}}{2A},0\right) = \frac{-3W_2^4+8BW_2^3}{192A^3} - \frac{PW_2^2}{8A^2}, \tag{9}$$

where $W_1 = -B+\sqrt{\Delta}$, $W_2 = B+\sqrt{\Delta}$.

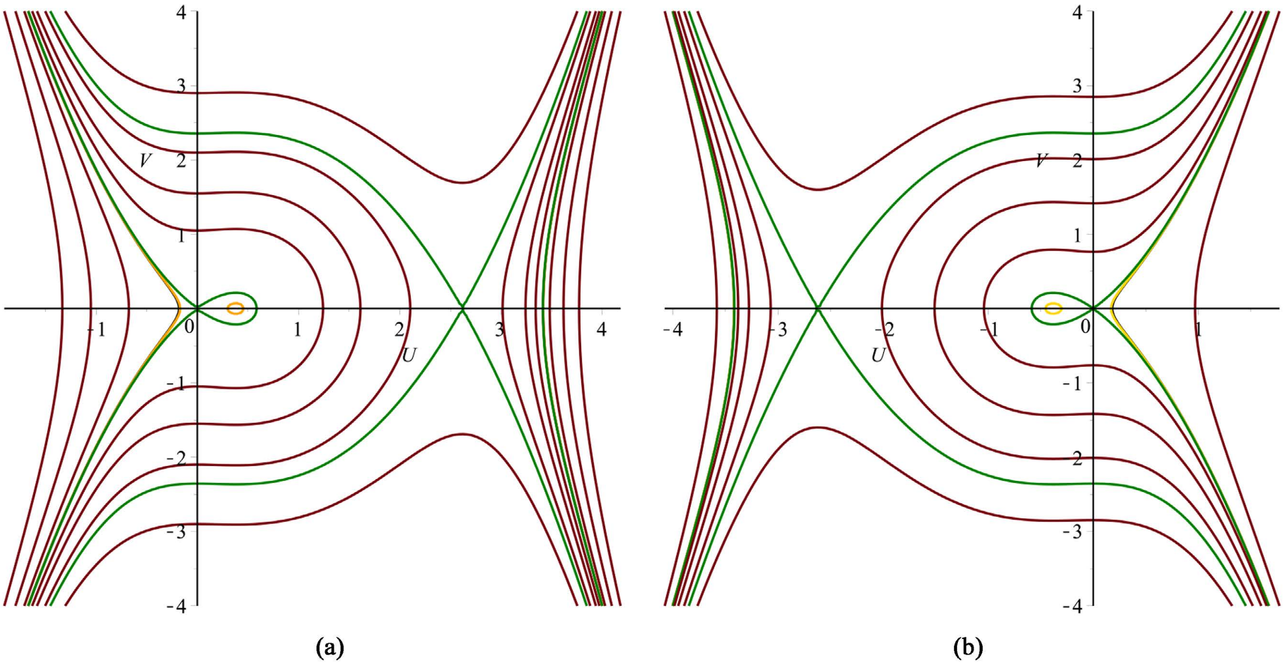

**Figure 2.** The phase portraits of the system (8). (a) $\Delta > 0, A > 0, B < 0, P > 0$; (b) $\Delta > 0, A > 0, B > 0, P > 0$.

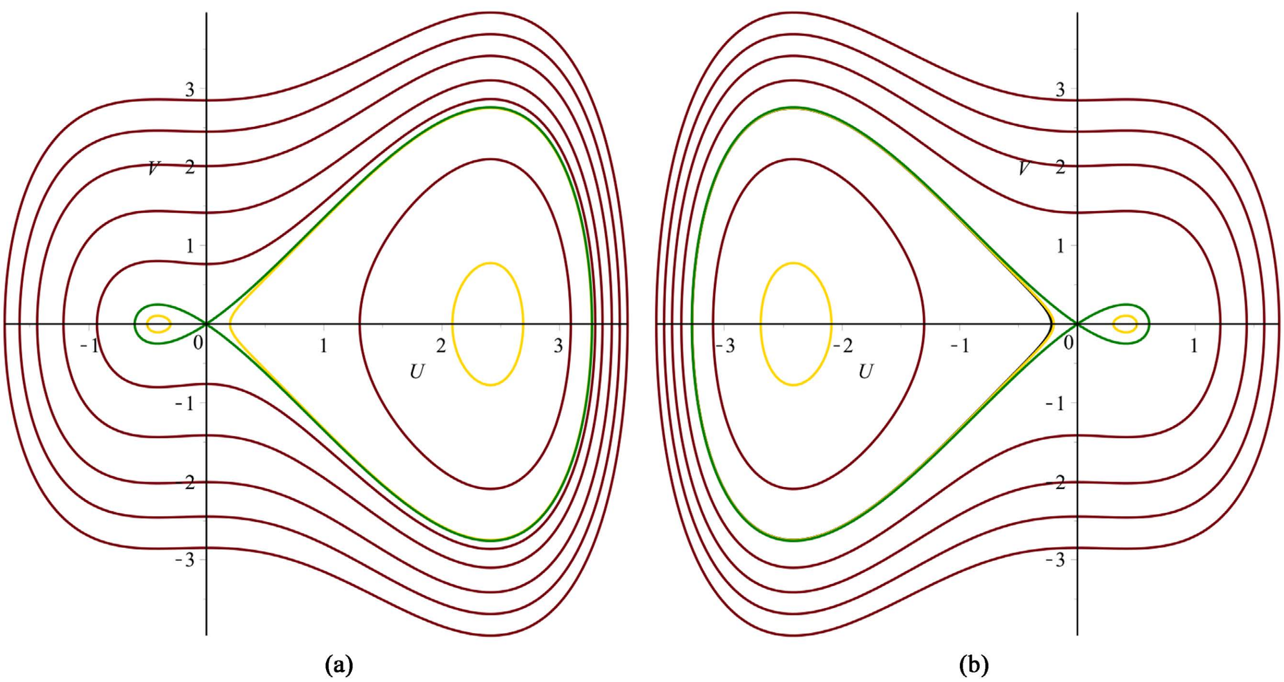

**Figure 3.** The phase portraits of the system (8). (a) $\Delta > 0, A < 0, B > 0, P > 0$; (b) $\Delta > 0, A < 0, B < 0, P > 0$.

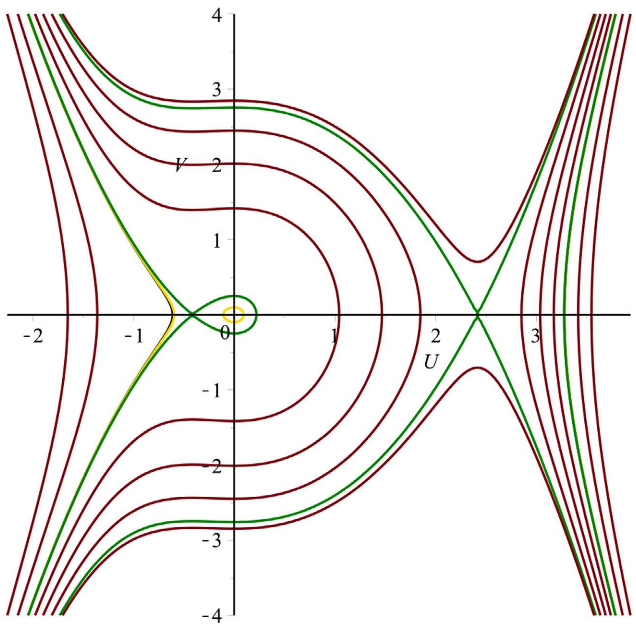


Figure 4. The phase portraits of the system (8). (a) $\Delta > 0, A > 0, B < 0, P < 0$; (b) $\Delta > 0, A > 0, B > 0, P < 0$.

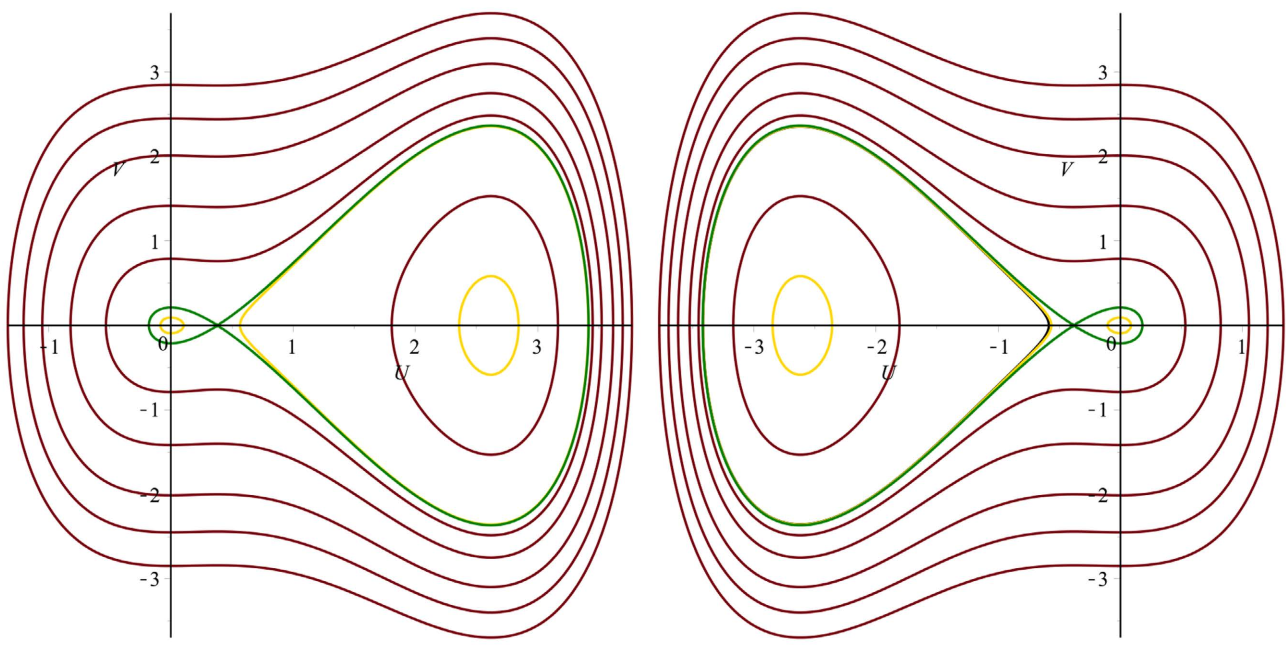


Figure 5. The phase portraits of the system (8). (a) $\Delta > 0, A < 0, B > 0, P < 0$; (b) $\Delta > 0, A < 0, B < 0, P < 0$.

### 4.1. Consider Case 1 in Section 3

By $\Delta = 0$, it obtains $PA > 0$.

(1) If $P > 0$, $A > 0$, corresponding to the homoclinic orbit $E_0(0,0)$ defined by $H(U,V) = h_0$ from (9), the Equation (1) has a solution of shown in Figure 1(a). By $H(U,V) = h_0 = 0$, it gets

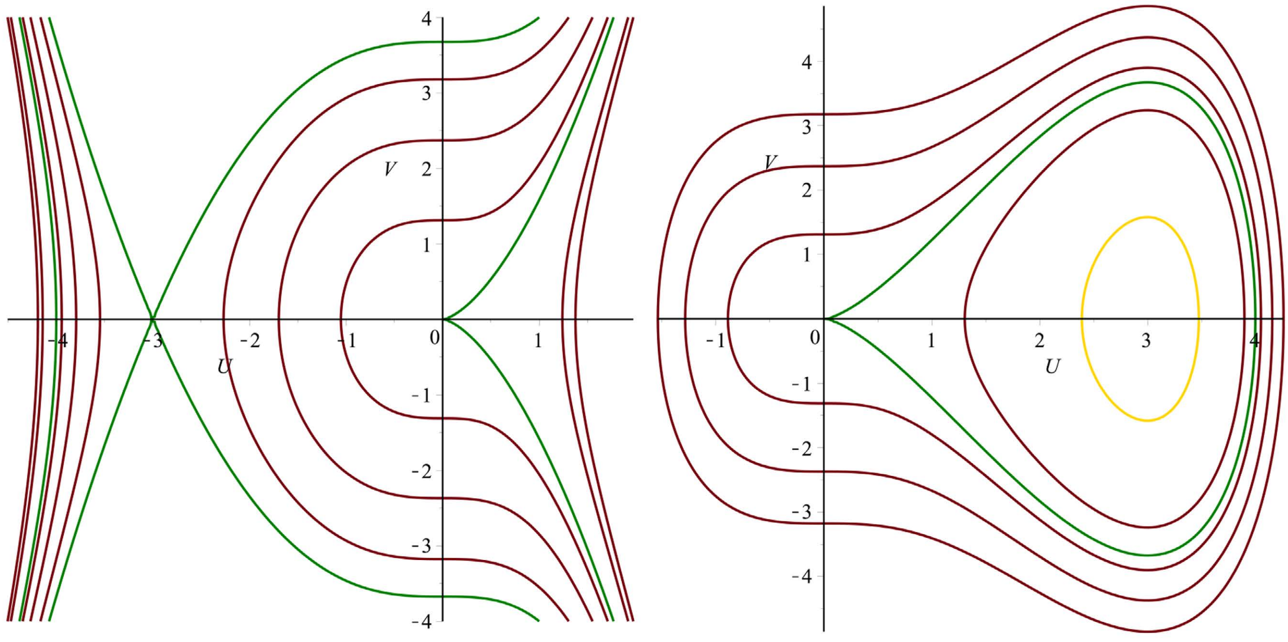


**Figure 6.** The phase portraits of the system (8). (a) $\Delta > 0, A > 0, P = 0$; (b) $\Delta > 0, A < 0, P = 0$.

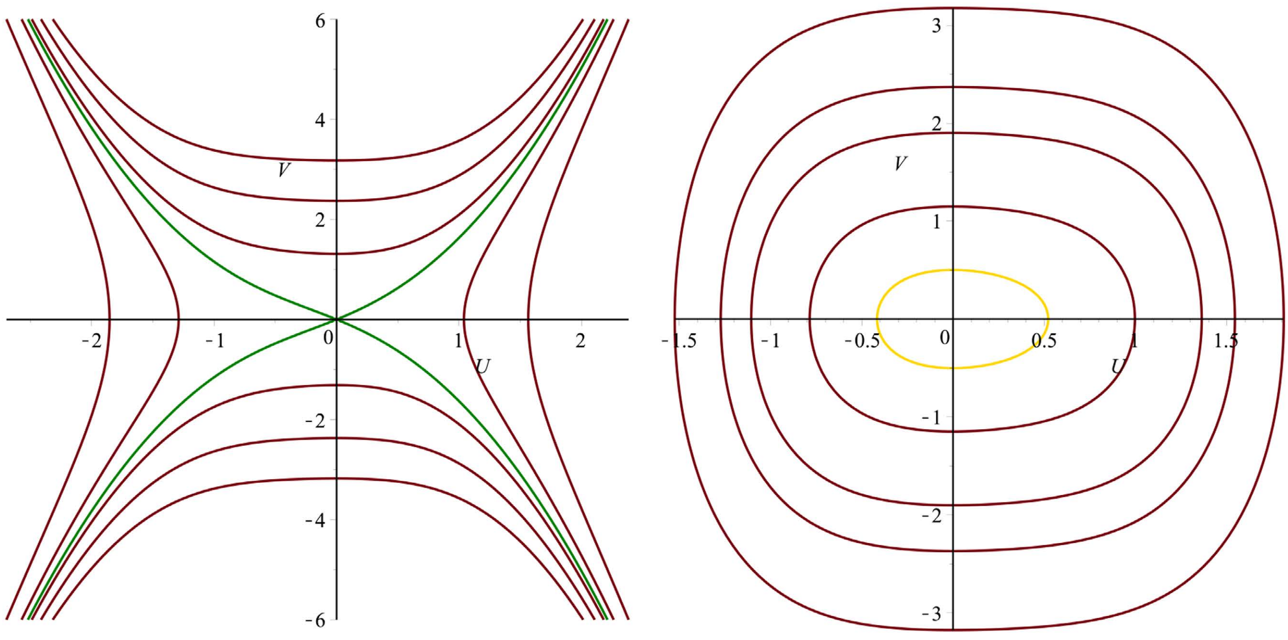


**Figure 7.** The phase portraits of the system (8). (a) $\Delta < 0, A > 0, P > 0$; (b) $\Delta < 0, A < 0, P < 0$.

$$V = \pm U\sqrt{\frac{A}{2}}\sqrt{\left(U + \frac{2B}{3A}\right)^2 + \frac{2PA}{9A^2}}. \tag{10}$$

Using the first equation of system (8) and equation (10), we get the following parameter expression

$$u(t,x)=\pm\frac{8A^2M_1\mathrm{e}^{-\frac{1}{3}\xi\sqrt{AM_1}}}{\mathrm{e}^{-\frac{2}{3}\xi\sqrt{AM_1}}A^2-72A^2M_1-24AB\mathrm{e}^{-\frac{1}{3}\xi\sqrt{AM_1}}+144B^2},\tag{11}$$

where $M_1=\frac{AP+2B^2}{A^2}$, $A=-\frac{s}{n^2+pk^2}$, $B=-\frac{r}{n^2+pk^2}$, $P=-\frac{q}{n^2+pk^2}$, and $\xi=kx-\frac{n}{\Gamma(1+\alpha)}t^\alpha$. The solution (11) is shown in **Figure 1(a)** with $A=1$, $B=2$, $C=1$.

2) If $P<0$, $A<0$, corresponding to the homoclinic orbit $E_0(0,0)$ defined by $H(U,V)=h_0$, the Equation (1) has a solution of shown in **Figure 1(b)**. By $H(U,V)=h_0=0$, it gets

$$V=\pm U\sqrt{-\frac{A}{2}}\sqrt{\left(U+\frac{2B}{3A}\right)^2+\frac{2PA}{9A^2}}.\tag{12}$$

By (8) and Equation (12), we get

$$u(t,x)=\pm\frac{8A^2M_1\mathrm{e}^{-\frac{1}{3}\xi\sqrt{-AM_1}}}{\mathrm{e}^{-\frac{2}{3}\xi\sqrt{-AM_1}}A^2-72A^2M_1-24AB\mathrm{e}^{-\frac{1}{3}\xi\sqrt{-AM_1}}+144B^2},\tag{13}$$

where $M_1=\frac{AP+2B^2}{A^2}$, $A=-\frac{s}{n^2+pk^2}$, $B=-\frac{r}{n^2+pk^2}$, $P=-\frac{q}{n^2+pk^2}$, and $\xi=kx-\left(\frac{n}{\Gamma(1+\alpha)}t^\alpha\right)$. The solution (13) is shown in **Figure 1(b)** with $A=-1$, $B=2$, $C=-1$.

### 4.2. Consider Case 2 in Section 3

1) If $P=0$, $A>0$, corresponding to the homoclinic orbit $E_0(0,0)$ defined by $H(U,V)=h_0$, Equation (1) has a solution of shown in **Figure 6(a)**. By $H(U,V)=h_0=0$, it infers

$$V=\pm U\sqrt{\frac{A}{2}}\sqrt{\left(U+\frac{4B}{3A}\right)U}.\tag{14}$$

Combining the first equation of system (8) and Equation (14), we have

$$u(t,x)=\frac{12B}{2\xi^2B^2-9A},\tag{15}$$

where $A=-\frac{s}{n^2+pk^2}$, $B=-\frac{r}{n^2+pk^2}$, and $\xi=kx-\frac{n}{\Gamma(1+\alpha)}t^\alpha$. The solution (15) is shown in **Figure 6(a)** with $A=1$, $B=3$.

2) If $P=0$, $A<0$, corresponding to the homoclinic orbit $E_0(0,0)$ defined by $H(U,V)=h_0$, the Equation (1) has a solution of shown in **Figure 6(b)**. By $H(U,V)=h_0=0$, it gets

$$V=\pm U\sqrt{-\frac{A}{2}}\sqrt{\left(U+\frac{4B}{3A}\right)U}.\tag{16}$$

Appling (8) and (16), we get

$$u(t,x) = -\frac{12B}{2\xi^2 B^2 + 9A}, \tag{17}$$

where $A = -\frac{s}{n^2 + pk^2}$, $B = -\frac{r}{n^2 + pk^2}$, and $\xi = kx - \frac{n}{\Gamma(1+\alpha)} t^\alpha$. The solution (17) is shown in **Figure 6(b)** with $A = -1$, $B = 3$.

3) If $P > 0$, $A > 0$ and $\Delta > 8PA$ or $P < 0$, $A < 0$ and $\Delta > 8PA$, corresponding to the homoclinic orbit $E_0(0,0)$ defined by $H(U,V) = h_0$, Equation (1) has the solution of shown in **Figure 2** or **Figure 5**. By $H(U,V) = h_0 = 0$, it obtains

$$V = \pm U \sqrt{\frac{A}{2}} \sqrt{\left(U + \frac{2B}{3A}\right)^2 + \frac{18PA - 4B^2}{9A^2}}. \tag{18}$$

It follows from (8) and (18), we obtain

$$u(t,x) = \frac{24A^2 M_2 e^{\mp\xi\sqrt{P}}}{\left(e^{\mp\xi\sqrt{P}}\right)^2 A^2 - 72A^2 M_2 - 8Ae^{\mp\xi\sqrt{P}} B + 16B^2},$$

where $M_2 = \frac{P}{A}$, $A = -\frac{s}{n^2 + pk^2}$, $B = -\frac{r}{n^2 + pk^2}$, $P = -\frac{q}{n^2 + pk^2}$, and $\xi = kx - \frac{n}{\Gamma(1+\alpha)} t^\alpha$.

4) If $P > 0$, $A < 0$ or $P < 0$, $A > 0$ corresponding to the homoclinic orbit $E_0(0,0)$ defined by $H(U,V) = h_0$, Equation (1) has the solution of shown in **Figure 3** or **Figure 4**. By $H(U,V) = h_0 = 0$, it gets

$$V = \pm U \sqrt{-\frac{A}{2}} \sqrt{\left(U + \frac{2B}{3A}\right)^2 + \frac{18PA - 4B^2}{9A^2}}. \tag{19}$$

Using the first equation of system (8) and Equation (19), we get the following parameter expression:

$$u(t,x) = \frac{24A^2 M_2 e^{\mp\xi\sqrt{-P}}}{\left(e^{\mp\xi\sqrt{-P}}\right)^2 A^2 - 72A^2 M_2 - 8Ae^{\mp\xi\sqrt{-P}} B + 16B^2},$$

where $M_2 = \frac{P}{A}$, $A = -\frac{s}{n^2 + pk^2}$, $B = -\frac{r}{n^2 + pk^2}$, $P = -\frac{q}{n^2 + pk^2}$, and $\xi = kx - \frac{n}{\Gamma(1+\alpha)} t^\alpha$.

5) If $P > 0$, $A > 0$ or $P < 0$, $A > 0$ corresponding to the homoclinic orbit $E_0(0,0)$ defined by $H(U,V) = h_0$ has the solution of shown in **Figure 2** or **Figure 4**. It follows from $H(U,V) = h_0 = 0$ that

$$V = \pm\sqrt{\frac{A}{2}} \sqrt{(U - U_4)(U - U_5)(U_6 - U)(U_7 - U)}. \tag{20}$$

The relation $U_4 < U_5 < U < U_6 < U_7$ holds on the $U$-axis. Therefore, by using the first equation of system (8) and equation (20), we get the following parameter expression

$$u(t,x)=1+\frac{U_7(U_5+U_6-U_7)-U_5U_6}{sn^2\left(\frac{|\xi|}{g}\sqrt{\frac{A}{2}}\right)(U_5-U_6)-U_5+U_7},$$

where $A=-s/(n^2+pk^2)$, $g=\frac{2}{\sqrt{(U_7-U_5)(U_6-U_4)}}$ and

$\xi=kx-\frac{n}{\Gamma(1+\alpha)}t^{\alpha}$.

### 4.3. Consider Case 3 in Section 3

1) If $P<0$, $A<0$, corresponding to the homoclinic orbit $E_0(0,0)$ defined by $H(U,V)=h_0$, Equation (1) has the solution of shown in Figure 7(b). By $H(U,V)=h_0=0$, it gets

$$V=\pm U\sqrt{-\frac{A}{2}}\sqrt{\left(U+\frac{2B}{3A}\right)^2+\frac{2PA}{9A^2}}. \tag{21}$$

Using the first equation of system (8) and Equation (21), we get the following parameter expression

$$u(t,x)=\pm\frac{8A^2M_1\mathrm{e}^{-\frac{1}{3}\xi\sqrt{-AM_1}}}{\mathrm{e}^{-\frac{2}{3}\xi\sqrt{-AM_1}}A^2-72A^2M_1-24AB\mathrm{e}^{-\frac{1}{3}\xi\sqrt{-AM_1}}+144B^2}, \tag{22}$$

where $M_1=\frac{AP+2B^2}{A^2}$, $A=-\frac{s}{n^2+pk^2}$, $B=-\frac{r}{n^2+pk^2}$, $P=-\frac{q}{n^2+pk^2}$,

and $\xi=kx-\frac{n}{\Gamma(1+\alpha)}t^{\alpha}$. The solution (22) is shown in Figure 7(b) with $A=-2$, $B=1$, $C=-1$.

(2) If $P>0$, $A>0$, corresponding to the homoclinic orbit $E_0(0,0)$ defined by $H(U,V)=h_0$, Equation (1) has the solution of shown in Figure 7(a). By $H(U,V)=h_0=0$, it gets

$$V=\pm U\sqrt{\frac{A}{2}}\sqrt{\left(U+\frac{2B}{3A}\right)^2+\frac{2PA}{9A^2}}. \tag{23}$$

Using the first equation of system (8) and Equation (23), we get the following parameter expression

$$u(t,x)=\pm\frac{8A^2M_1\mathrm{e}^{-\frac{1}{3}\xi\sqrt{AM_1}}}{\mathrm{e}^{-\frac{2}{3}\xi\sqrt{AM_1}}A^2-72A^2M_1-24AB\mathrm{e}^{-\frac{1}{3}\xi\sqrt{AM_1}}+144B^2}, \tag{24}$$

where $M_1=\frac{AP+2B^2}{A^2}$, $A=-\frac{s}{n^2+pk^2}$, $B=-\frac{r}{n^2+pk^2}$, $P=-\frac{q}{n^2+pk^2}$,

and $\xi=kx-\frac{n}{\Gamma(1+\alpha)}t^{\alpha}$. The solution (24) is shown in Figure 7(a) with

$A = 2$, $B = 1$, $C = 1$.

## 5. Conclusion

In conclusion, we obtained the phase portraits of the traveling wave system by using the fractional complex transformation and the dynamical system method [19] [20]. Moreover, we construct all possible accurate traveling wave solutions of Equation (1) under different parameter conditions.

## Data Availability

The data used to support the findings of this study are available from the corresponding author upon request.

## Conflicts of Interest

The authors declare no conflicts of interest regarding the publication of this paper.

## References

[1] Yan, Z. and Zhang, H. (1999) Explicit and Exact Solutions for the Generalized Reaction Duffing Equation. *Communications in Nonlinear Science and Numerical Simulation*, **4**, 224-227. https://doi.org/10.1016/S1007-5704(99)90010-2

[2] Tian, B. and Gao, Y. (2002) Observable Solitonic Features of the Generalized Reaction Duffing Model. *Zeitschrift für Naturforschung A*, **57**, 39-44. https://doi.org/10.1515/zna-2002-9-1004

[3] Chen, Y., Yan, Z. and Zhang, H. (2002) Exact Solutions for a Family of Variable-Coefficient "Reaction-Duffing" Equations via the Bäcklund Transformation. *Theoretical and Mathematical Physics*, **132**, 970-975. https://doi.org/10.1023/A:1019663425564

[4] Eslami, M., Vajargah, B.F., Mirzazadeh, M., *et al.* (2014) Application of First Integral Method to Fractional Partial Differential Equations. *Indian Journal of Physics*, **88**, 177-184. https://doi.org/10.1007/s12648-013-0401-6

[5] Guner, O., Bekir, A. and Korkmaz, A. (2017) Tanh-Type and Sech-Type Solitons for Some Space-Time Fractional PDE Models. *The European Physical Journal Plus*, **132**, 92-103. https://doi.org/10.1140/epjp/i2017-11370-7

[6] Huang, D. and Zhang, H. (2005) The Extended First Kind Elliptic Subequation Method and Its Application to the Generalized Reaction Duffing Model. *Physics Letters A*, **344**, 229-237. https://doi.org/10.1016/j.physleta.2005.06.070

[7] Arnous, A.H. and Mirzazadeh, M. (2014) Backlund Transformation of Fractional Riccati Equation and Its Applications to the Spacetime FDEs. *Mathematical Methods in the Applied Sciences*, **38**, 4673-4678. https://doi.org/10.1002/mma.3371

[8] Sonmezoglu, A. (2015) Exact Solutions for Some Fractional Differential Equations. *Advances in Mathematical Physics*, **2015**, Article ID: 567842. https://doi.org/10.1155/2015/567842

[9] Rezazadeh, H., Korkmaz, A., Eslami, M., *et al.* (2018) Traveling Wave Solution of Conformable Fractional Generalized Reaction Duffing Model by Generalized Projective Riccati Equation Method. *Optical and Quantum Electronics*, **50**, 150-162. https://doi.org/10.1007/s11082-018-1416-1

[10] Kim, J.J. and Hong, W.P. (2004) New Solitary-Wave Solutions for the Generalized Reaction Duffing Model and Their Dynamics. *Zeitschrift für Naturforschung A*, **59**, 721-728. https://doi.org/10.1515/zna-2004-1101

[11] Dai, C. and Xu, Y. (2015) Exact Solutions for a Wick-Type Stochastic Reaction Duffing Equation. *Applied Mathematical Modelling*, **39**, 7420-7426. https://doi.org/10.1016/j.apm.2015.03.019

[12] Jafari, H., Tajadodi, H., Baleanu, D., *et al.* (2013) Fractional Subequation Method for the Fractional Generalized Reaction Duffing Model and Nonlinear Fractional Sharma-Tasso-Olver Equation. *Central European Journal of Physics*, **11**, 1482-1486. https://doi.org/10.2478/s11534-013-0203-7

[13] Zeng, Z., Liu, X., Zhu, Y., *et al.* (2022) New Exact Traveling Wave Solutions of (2+1)-Dimensional Time-Fractional Zoomeron Equation. *Journal of Applied Mathematics and Physics*, **10**, 333-346. https://doi.org/10.4236/jamp.2022.102026

[14] Wang, S., Yu, H., Dai, C., *et al.* (2020) Bosonization Approach and Novel Traveling Wave Solutions of the Superfield Gardner Equation. *Journal of Applied Mathematics and Physics*, **8**, 443-455. https://doi.org/10.4236/jamp.2020.83034

[15] Aljahdaly, N.H., Shah, R., Agarwal, R.P., *et al.* (2022) The Analysis of the Fractional-Order System of Third Order KdV Equation within Different Operators. *Alexandria Engineering Journal*, **61**, 11825-11834. https://doi.org/10.1016/j.aej.2022.05.032

[16] Zhang, L., Feng, M., Agarwal, R.P., *et al.* (2022) Concept and Application of Interval-Valued Fractional Conformable Calculus. *Alexandria Engineering Journal*, **61**, 11959-11977. https://doi.org/10.1016/j.aej.2022.06.005

[17] Al-Sawalha, M.M., Agarwal, R.P., Shah, R., *et al.* (2022) A Reliable Way to Deal with Fractional-Order Equations that Describe the Unsteady Flow of a Polytropic Gas. *Mathematics*, **10**, Article No. 2239. https://doi.org/10.3390/math10132293

[18] Agarwal, R.P. and Hristova, S. (2022) Impulsive Memristive Cohen-Grossberg Neural Networks Modeled by Short Term Generalized Proportional Caputo Fractional Derivative and Synchronization Analysis. *Mathematics*, **10**, Article No. 2355. https://doi.org/10.3390/math10132355

[19] Zhu, W., Xia, Y. and Zheng, B. (2022) Bifurcations and Traveling Wave Solutions of Lakshmanan-Porsezian-Daniel Equation with Parabolic Law Nonlinearity. *International Journal of Bifurcation and Chaos*, **32**, Article ID: 2250126. https://doi.org/10.1142/S0218127422501267

[20] Li, J. and Liu, Z. (2002) Traveling Wave Solutions for a Class of Nonlinear Dispersive Equations. *Chinese Annals of Mathematics*, **23**, 397-418. https://doi.org/10.1142/S0252959902000365

[21] Khalil, R., Horani, M.A., Yousef, A., *et al.* (2014) A New Definition of Fractional Derivative. *Journal of Computational and Applied Mathematics*, **264**, 65-70. https://doi.org/10.1016/j.cam.2014.01.002

[22] Li, Z. and He, J. (2010) Fractional Complex Transform for Fractional Differential Equations. *Mathematical and Computational Applications*, **15**, 970-973. https://doi.org/10.3390/mca15050970

[23] Liang, J., Tang, L., Xia, Y., *et al.* (2020) Bifurcations and Exact Solutions for a Class of mKdV Equations with the Conformable Fractional Derivative via Dynamical System Method. *International Journal of Bifurcation and Chaos*, **30**, Article ID: 2050004. https://doi.org/10.1142/S0218127420500042